Influence of antibody Fab charge, hydrophobicity, and hydrodynamic size on vitreous pharmacokinetics in rabbits

BY

Kathryn Wang

Submitted to the graduate degree program in Pharmaceutical Chemistry Department and the Graduate Faculty of the University of Kansas in partial fulfillment of the requirements for the degree of Master of Science.

_____

Professor: Jeff Krise

_____

Professor: John Stobaugh

_____

Adviser: Robert Kelley

Date Defended: 8/23/2017

The Thesis Committee for Yue Wang certifies that this is the approved version of the following thesis:

Influence of antibody Fab charge, hydrophobicity, and hydrodynamic size on vitreous pharmacokinetics in rabbits

_____

Professor: Jeffrey Krise

_____

Adviser: Robert Kelley

Date approved: 9/6/2017

ABSTRACT

A better understanding of the molecular attributes contributing to vitreal elimination half-life could enable the design of improved therapeutics for the treatment of human posterior segment ocular disease. Here we have used pharmacokinetics (PK) studies in rabbits to probe the contribution of electrostatic charge, hydrophobicity, and hydrodynamic size to vitreal clearance of antibody fragments (Fabs). Comparing Fabs of diverse binding targets, we find that vitreal half-life is not strongly correlated with measured isoelectric point (pI) or the hydrophobicity index (HI) of the variable domain unit (Fv) calculated from the amino acid sequence. We completed two systematic studies of molecule charge and hydrophobicity by determining the vitreal half-life of variants of ranibizumab. Charge or hydrophobicity was altered through introduction of amino acid changes in two of the hypervariable regions of the light chain. Equivalent vitreal pharmacokinetics were observed for ranibizumab and these variants with pIs in the range 6.8 – 10.2 and Fv HI varied in the range 1090-1296. Finally, a previously observed linear dependence between vitreal half-life and hydrodynamic radius, determined using light scattering measurements, has been extended to a broader range. These results indicate that diffusive properties of antibody Fabs, as quantified by the hydrodynamic radius, make a key contribution to vitreal elimination whereas minor or negligible contributions arise from differences in charge or hydrophobicity in the ranges tested in these studies.

ACKNOWLEDGEMENTS

This thesis was written through contributions of the following colleagues: Susan Crowell and Leslie Dickmann designed and analyzed the pharmacokinetic studies. Whitney Shatz, led and completed the contribution of antibody hydrodynamic size to vitreal clearance study. Devin Tesar, experiment and study design advisor. Robert Kelley, the thesis research advisor and the Ocular PK research advisor.

TABLE OF CONTENTS **PAGE**

LIST OF FIGURES

Figure: Page

LIST OF TABLES

1. INTRODUCTION

Age-related macular degeneration (AMD) is a progressive chronic disease of the central retina with significant consequences for visual acuity[1]. AMD has two inter-related forms: wet and dry. Wet, also known as neovascular, AMD accounts for approximately 10% of all cases. It is characterized by excessive growth of blood vessels from the choroid behind the retina, and can cause severe visual impairment. Visual acuity for patients afflicted with wet AMD is often improved by treatment with anti-VEGF agents such as Lucentis® (ranibizumab)[2, 3]. Ranibizumab, the Fab fragment of an engineered anti-VEGF antibody, is also efficacious and approved for the treatment of retinal vein occlusion (RVO) and diabetic macular edema (DME). Dry AMD accounts for the remaining 90% of cases, currently has no treatment options, and can be a precursor to wet AMD. Advanced dry AMD can result in significant retinal damage, including geographic atrophy[4], with irreversible vision loss. Lampalizumab, an anti-factor D (fD) antibody Fab fragment is in clinical development at Genentech for the treatment of geographic atrophy, secondary to AMD.

The vitreous is the largest structure in the eye, taking up roughly 80 % of its volume[21]. In humans, the vitreous is approximately four mL in volume comprising 98 % water, soluble and insoluble proteins, and proteoglycans. The vitreous has a gel-like structure formed

from collagen (50-100 μg/mL) and hyaluronan (HA) (100-400 μg/mL)[22]. Collagen, primarily type II collagen, is an important structural protein in the vitreous. Collagen fibers are organized as a triple helix of three alpha chains to form a loose network that provides the ocular tissue with tensile strength and maintains the gel-like state[21, 22]. HA, a high molecular weight linear polymer with a random coil conformation, composed of a disaccharide repeat of glucuronic acid and N-acetyl glucosamine, fills the space between the collagen fiber network and provides swelling pressure to resist compression force and maintain the vitreous gel-like structure[21].

Upon intravitreal injection, elimination of drug molecules from the vitreous cavity can be generalized by two routes before outflow to the systemic blood circulation[30] (**Figure 1**): the anterior route through the aqueous humor via ciliary body and zonules followed by drainage to the lymphatic system through normal aqueous humor outflow, and the posterior route by crossing the blood-ocular barriers through choroidal vasculature. Given the dimensions of the anterior chamber, and the rate of fluid production[13], the entire contents of the aqueous humor are turned over in a few hours. In either route, the diffusivity of a drug molecule can be influenced by the interactions between the molecule and the collagen-HA network of the vitreous humor. Although some quantitative studies of small molecule vitreal pharmacokinetics (PK) have been performed[19], the impact of

physicochemical properties such as hydrodynamic size, electrostatic charge, and hydrophobicity on the vitreal PK of protein therapeutics are not well understood.

Figure 1. Scheme of the various routes of ocular drug administration and the anatomy of the eye[30].

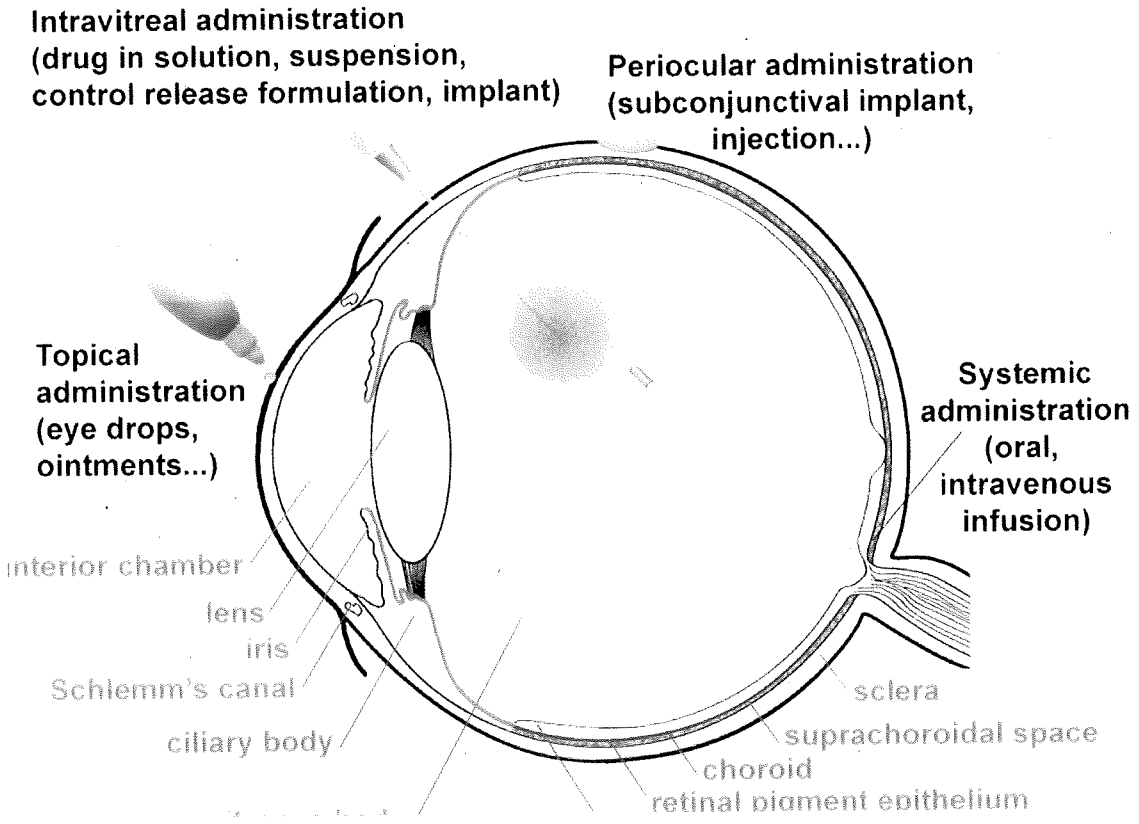

Intravitreal injection is the preferred route for ocular drug delivery of protein therapeutics to the posterior segment of the eye. Due to the relatively rapid clearance of protein drugs

from the eye following administration, maximal efficacy requires frequent dosing, typically monthly or bi-monthly. In order for some molecules to be efficacious, they must be delivered to the retina by passing the inner limiting membrane (ILM), the membrane layer separating the retina and the vitreous[20]. Studies with ^{125}I-labeled full-length antibodies and antibody fragments (Fabs) in Rhesus Monkeys have suggested a molecular weight dependence of retinal penetration[15]. Moreover, the high dense gel-like collagen-HA meshwork in vitreous is known as a size-dependent permeable membrane[24]. Studies with bovine vitreous tissue ex vivo confirmed that the collagen-HA meshwork is highly permeable for non-adhesive nanoparticles smaller than 510 nm in hydrodynamic radius (R_H), but impermeable to nanoparticles greater than 1190 nm in R_H regardless of surface chemistry[23].

A recent study using amphiphilic polymeric nanoparticles demonstrated that the movement of intravitreal nanoparticles depended upon the surface charge[16]. The study revealed that the HA anionic nanoparticles with a 213.4 ± 10.3 nm of size and a zeta potential of −26.2 ± 4.0 mV diffused more freely through the collagen fibril-HA network in the vitreous and showed efficient penetration across the retina. On the other hand, the glycol chitosan (GC) cationic nanoparticles with a similar size at 229.1 ± 8.7 nm and a zeta potential of +16.4 ± 3.2 mV diffused slower in the vitreous, and could not penetrate into the deeper retinal structures and accumulated on the ILM. Similarly, Mahaling et al. used surface

modification to show that hydrophobic core nanoparticles with different hydrophilic shells displayed different ocular permeability[17]. These studies suggest that, aside from hydrodynamic size, charge and hydrophobicity may impact vitreal clearance and ocular partitioning.

These results suggest molecular charge and hydrophobicity may influence the ocular PK and distribution of soluble macromolecules. By studying these properties, we could better understand the factors that influence ocular PK and potentially engineer therapeutic molecules with more desirable intravitreal PK properties[5], such as better retinal partitioning, slower vitreal clearance, and lower systemic exposure[3]. This could help reduce the treatment burden to patients by enabling less frequent dosing and increase patient convenience and compliance.

Engineering antibody Fabs to have improved ocular pharmacokinetics is one strategy to allow less frequent dosing. As part of an effort to accomplish this goal, we have undertaken studies to assess molecule attributes affecting ocular clearance. Our hypothesis is that hydrodynamic size is a key determinant of ocular clearance whereas only minor or negligible contributions are made by variation in molecule charge or hydrophobicity. In these studies, variants of ranibizumab that vary the charge or the hydrophobicity were

carefully designed and their ocular pharmacokinetics were determined in rabbit. A previously established linear relationship between vitreal half-life and hydrodynamic radius[5] has been expanded to a larger size range. Results of these studies are incorporated into a model for estimating ocular pharmacokinetic behavior on the basis of molecule physiochemical properties.

2. MATERIALS AND METHODS

2.1 ANTIBODY FAB FRAGMENTS

The antibody Fab fragments designed for the studies are described in **Table 1**. Antibody Fabs designated for intravitreal injection were formulated in PBS pH 7.4, at 10 mg/mL such that a 50 µL injection delivered a 0.5 mg dose. Endotoxin levels were determined using Y57: LAL assay (Genentech Analytical Operations) and kept below 0.1 endotoxin units (EU)/eye. Values for isoelectric point (pI) were determined by imaged capillary isoelectric focusing (iCIEF) as described by Salas-Solano et al.[8] For some Fabs, only a calculated, rather than measured pI, was determined using the "SMACK" algorithm developed by T. Patapoff and V. Sharma (Genentech, Inc.). Hydrophobicity of the antibody Fv domains was calculated from the amino acid sequence using the SMACK program and the Eisenberg hydrophobicity scale[25].

Table 1. Properties of ranibizumab Fab variants used for rabbit pharmacokinetic studies

Molecule	pI (theor.)	FvHI	AUC_inf/D (µg/mL*d)	Half-life (days)	CL (ml/day)	Vss (mL)
RBZ +7	10.2	1160	3630	3.0	0.27	**1.0**
RBZ -3	6.8	1009	2890	3.0	0.34	**1.2**
RBZ less hydro.	8.9	1165	2530	3.3	0.40	**1.9**
RBZ more hydro.	9.1	1296	2550	3.3	0.39	**1.8**
RBZ _WT (n=12)	**8.9**	**1212**	**3610 ± 1370**	**3.4 ± 0.7**	**0.3 ± 0.1**	**1.5 ± 0.5**

2.2 Analytical hydrophobic interaction chromatography (HIC)

Retention time on a 2.1x100 mm ProPacHIC-10 column was determined for the selected antibody Fabs using analytical HIC. Mobile phase A consisted of 2.5 M ammonium sulfate, 25 mM sodium phosphate pH 6.5 and mobile phase B was 25 mM sodium phosphate pH 6.5, 25% isopropanol. The column was equilibrated in 100% A at a flow rate of 0.2 mL/min and 5 µg of Fab solutions in 90% mobile phase A were injected per analysis. Fabs were eluted with a linear gradient (3%/min) of 0-75% buffer B and detected by UV absorbance at 280nm wavelength.

2.3 Production and characterization of ranibizumab charge variants

Mutations were introduced into the ranibizumab expression plasmid (Y0317) by site-directed mutagenesis using the QuikChangeII® (Agilent) mutagenesis kit following the protocol supplied by the manufacturer. Oligonucleotide primers specifying the required codon changes were synthesized by the Genentech oligonucleotide synthesis lab (oligo can be ordered directly from Integrated DNA Technologies-IDT) . Plasmids with designed changes were identified and confirmed by DNA sequencing[28] at Genentech. For small-scale expression and purification, DNA was transformed into E. coli strain 64B4. Single colonies were picked into 5 mL LB media (media prep code A2008) containing 50 µg/mL carbenicillin (media prep code A3232) and grown overnight in 14 mL culture tubes with shaking at 200 RPM in an Innova incubator at 37 °C. These cultures were used to inoculate 250 mLs of complete soy crap media (media prep code A4564), 50 µg/mL carbenecillin, in a 1 L baffled shake flask. Cultures were grown overnight at 30 °C with shaking at 200 RPM and then harvested by centrifugation. The cell pellets were lysed using PopCulture media (invitrogen), and Fabs were purified on Gravitrap Protein G columns (GE Healthcare), following protocols supplied by the manufacturers. For larger scale production of Fabs, cell paste from 10 L fermentation[29] of transformed cells was provided by Genentech fermentation group. Cell paste was suspended in extraction buffer and homogenized using a microfluidizer.. Fabs were captured by immunoaffinity chromatography on Protein G-

Sepharose with an elution buffer of 0.1M acetic acid, pH 2.75. The low pH eluate was buffer exchanged into 25mM NaOAc at pH 5.0 and further purified by cation exchange chromatography on a Hitrap SP HP pre-packed column. Identities of the purified proteins were confirmed by mass spectroscopy and the pooled fractions were concentrated to 10 mg/mL and exchanged into PBS buffer via ultrafiltration / diafiltration with Amicon 10kD MW centrifugal filters.

VEGF-binding affinities were determined by surface plasmon resonance (SPR) measurements on a Biacore ® T200 instrument (GE Healthcare) using a series S, CM5 carboxymethylated dextran sensor chip. The sensor chip was first activated with amine-coupling reagents. VEGF was covalently immobilized at varied coupling density through injection of different concentrations of VEGF solutions (10 mM sodium acetate, pH 5.0) onto separate flow cells of the activated chip. Finally, all the unreacted amine-coupling sites were blocked with 1 M ethanolamine. Sensorgrams were collected for injections of 30 µL aliquots of 15 solutions of anti-VEGF antibody Fabs varied in concentration from 5 pM to 10 nM with the flow rate set at 10 µL/min. Antibody bound to specific antigen was determined from the response signal near the end of the sample injection. Bound antibody was eluted at the end of each binding cycle through injection of 30 µL of 10 mM Gly-HCl pH 2.1 to cause dissociation of the antibody-antigen complex. Kinetics constants and equilibrium

dissociation constant (K_D) were calculated from these data using BIAEvaluation software (GE Healthcare)

The isoelectric points (pIs) were evaluated by imaged capillary isoelectric focusing (icIEF) using ProteinSimple iCE280. icIEF is a highly resolving electrophoretic method that can separate peptides and proteins on the basis of their pI, and resolve proteins that differ by 0.01 pI units. Prior to analysis, samples were diluted with ampholyte mixture to 1.25mg/mL. The ampholyte mixture (2000 µL) was comprised of 237 µL of ddH2O, 700 µL of 1% methylcellulose, 1000 µL of 5M Urea, 19 µL of 5-8 ampholyte, 44 µL of 8-10.5 ampholyte, and an appropriate amount of pI markers. Each sample injection was 100 µL. Upon filling a capillary with a co-mix of analyte and ampholyte, the cathodic side is placed in a solution of NaOH, while the anodic side was placed in a solution of H_3PO_4. The total run time per sample was about 30mins, and the status of the isoelectric focusing was monitored by current measurements in microamps (µA). Triplicate pI measurements were obtained for WT and charge variants of ranibizumab. The pI 5.5 and 9.77 markers were used for ranibizumab WT and RBZ-3 samples, while pI 9.22 marker was used for RBZ+7 because the pI 9.77 marker will overlap with the main peak of RBZ+7.

SE-HPLC (Size Exclusion High-performance Liquid Chromatography) was performed using an Agilent 1200 series HPLC system equipped with a diode array detector (DAD). The column,

TOSOH TSK-Gel Super SW2000 (4.6 mm × 300 mm, Tosoh, cat. # 18675), with common bead size of 4 µm, was utilized to differentiate proteins by different molecular size at room temperature. The SE-HPLC method runs isocratically at 0.2 mL/min for a total of 30 minutes with 0.20 M K3PO4, 0.25 M KCl, pH 6.2 as the mobile phase. Samples were diluted to between 0.2-1 mg/mL in Phosphate buffered saline with polysorbate 20 and sodium azide (PBSTN - 137 mM NaCl, 2.7 mM KCl, 10 mM Na2HPO4·2H20, 2 mM KH2PO4, 0.01% (w/v) polysorbate 20, 0.02% (w/v) sodium azide) and a 100 µL of sample were injected per analysis. Absorbance at 280 nm was used for detection.

IEC (Ion Exchange High-performance Liquid Chromatography) was performed using an Agilent 1200 series HPLC system with two Dionex (Sunnyvale, CA) ProPac SAX-10 (2 mm × 250 mm) strong anion-exchange columns in series. Mobile phase A was pH 3.55 (2.4 mM Tris, 1.5 mM Imidazole, 11.1 mM Piperazine) and mobile phase B was pH 11.0 (2.4 mM Tris, 1.5 mM Imidazole, 11.1 mM Piperazine). A 60-minute linear gradient was used, going from 0% to 100% mobile phase B. Samples were diluted to approximately 0.05 mg/mL in phosphate buffered saline (PBS) and 100 µL of sample was injected. Absorbance at 280 nm was used for detection using the diode array detector.

2.4 Production and characterization of ranibizumab hydrophobic variants

The DNA sequence of the ranibizumab hydrophobic variants were designed using the

GSeqEdit software and assembled by gene synthesis (Genewiz). Fabs were expressed and purified on Protein G followed by cation exchange as described above for charge variants. Final endotoxin removal steps were performed to ensure the endotoxin levels were kept below 0.1 EU/eye. In order to maximize the endotoxin clean up efficiency and recovery, the purified proteins were first filtered through a 0.2µm, 25mm Pall Mustang E arodisc filter, where about 90% of the endotoxin was removed. The filtering step was performed on the protein solution using an auto-injector with a 30 mL Luerlok syringe at a rate of 0.5 mL/hour, and followed by a 10 mL 25mM NaOAc at pH 5.0 buffer cleanup step at a rate of 2 mL/hour to enhance protein recovery. The filtered protein solutions were further cleaned by cation exchange chromatography on a Hitrap SP HP pre-packed column with an overnight 0.1 % Triton 110 / Triton 114 wash[26] at a low-flow rate. Identities of the purified proteins were confirmed by mass spectroscopy, and the pooled fractions were concentrated to 10 mg/mL, and exchanged into PBS buffer, via diafiltration. The endotoxin levels of the final protein solutions were determined using Y57: LAL assay[27] (Genentech Analytical Operations).

2.5 Pharmacokinetic studies on ranibizumab variants

Two pharmacokinetic (PK) studies on ranibizumab variants were performed to assess the impact of molecule attributes on ocular clearance, with the first study focused on charge (testing articles: ranibizumab WT, RBZ +7 and RBZ -3), and the second study focused on

hydrophobicity (testing articles: ranibizumab WT, less and more hydrophobic variants).

For each pK study, 30 Naïve New Zealand White (NZW) rabbits (male animals, 2.4-3.2 kg and approximately 4 months of age at the time of dosing, obtained from Charles River Laboratories) were assigned to dose groups and dosed with the test articles at Genentech. All the dose groups were administered via a single bilateral intravitreal injection to animals as outlined in the experimental design below and observed for up to 18 days.

Topical antibiotic (tobramicin ophthalmic ointment) was applied to both eyes twice on the day before treatment, immediately following the injection, and twice on the day following the injection, with the exception of animals sent to necropsy on Days 1 and 2. Prior to dosing, mydriatic drops (1% tropicamide) were applied to each eye for full pupil dilation. Animals were sedated with isoflurane/oxygen gas prior to and during the procedure. Alcaine (0.5%) was also applied to each eye prior to injection. The conjunctivae was flushed with benzalkonium chloride (ZephiranTM) diluted in sterile water, U.S.P. to 1:10,000 (v/v).

Syringes were filled under a laminar flow hood immediately prior to dosing. Fabs were administered by a single 50 µL intravitreal injection to each eye. Doses were administered by a board-certified veterinary ophthalmologist using sterilized 100 µL Hamilton Luer Lock

syringes with a 30-gauge x 1/2" needle. In order to mimic clinical dosing, eyes were dosed in the infero-temporal quadrants, i.e. in 5 o'clock and 7 o'clock positions for the left and right eyes, respectively (when facing the animal). The eyes were examined by slit-lamp biomicroscopy and/or indirect ophthalmoscopy immediately following treatment.

All animals underwent exsanguination by incision of the axillary or femoral arteries following anesthesia by intravenous injection of sodium pentobarbital. At 0.125, 2, 7, 15, and 18 days post-injection, aqueous humor, vitreous humor and retina tissue were collected, snap frozen in liquid nitrogen and stored at -80°C. Retinal tissues were homogenized using an Omni bead ruptor. Concentrations of Fabs in tissues were determined using a "VEGF-coat" ELISA[7]. Values below the LLOQ were not used in pharmacokinetic analysis or for graphical or summary purposes. Pharmacokinetic parameters were determined by non-compartmental analysis with nominal time and dose (Phoenix WinNonlin, Pharsight Corp, Mountain View, CA).

Pharmacokinetic parameters reported are as follows:

Cmax = Maximum observed concentration

AUC_{all} = area under the vitreous concentration versus time curve from Time 0 to C_{last}

CL = clearance = Nominal dose (mg/kg) /AUC_{inf}

$t_{1/2,\ elim}$ = half-life associated with the terminal phase [ln(2)/λz]

Vss = volume of distribution at steady-state.

3. RESULTS

The ranibizumab variants for which pharmacokinetic data have been determined upon intravitreal injection in rabbits have been compiled in **Table 1** along with the molecular properties of pI and calculated hydrophobicity. Since the variants differ by changes only in the variable domain unit (Fv), the charge and hydrophobic index (HI) calculations are focused on the Fv, but calculated and measured isoelectric point (pI) values are for the intact Fab. Multiple pharmacokinetic studies (n=12) have been conducted with ranibizumab WT, and yield a mean vitreal half-life in rabbit of 3.4 ± 0.7 days. The vitreal half-life for the remainder of the ranibizumab variants was determined from a single pharmacokinetic study and revealed a range in vitreal half-life of 3.0-3.3 days, which is within the variability of historical ranibizumab WT readings.

3.1 Ranibizumab charge variants production and characterization

Examination of the high-resolution crystal structure of the ranibizumab: VEGF complex[9] suggested that two CDRs, CDR-1 (CDR-L1) and CDR-2 (CDR-L2) of the light chain, are non–antigen –contacting regions in ranibizumab. This is consistent with results of mutagenesis studies showing that alanine mutants of individual residues in these two CDRs do not perturb VEGF-binding affinity. In order to minimize structure and conformational alterations due to introduction of charged substitutions, and to ensure the variants have sufficient antigen-binding affinity for detection using assays employed in pharmacokinetic studies, mutations were only introduced at solvent exposed sites in CDR-L1 and CDR-L2. Two positive and three negative ranibizumab charge variants with different combination of mutations resulted from this design process. The CDR-L1 and CDR-L2 sequences of ranibizumab WT and charge variants are provided in **Table 2**. Since only one positive and one negative variant can be selected for pharmacokinetic studies, multiple evaluation studies were conducted to determine the most suitable charge variants. These variants, RBZ-3 and RBZ+7, were chosen since both charge variants inherited strong VEGF-binding affinities and also provide a sufficient range (10 units) of charge variation. The electrostatic surfaces of the Fv portion of these Fabs were modeled onto the structure of ranibizumab WT using PyMOL v1.7.0.5 (Schrödinger, LLC) and are displayed in **Figure** 2. Since charge is introduced into adjacent CDRs a negative or positive charge "patch" is produced rather than a delocalized charge region.

Table 2. Properties of ranibizumab Fab variants designed for rabbit pharmacokinetic studies

Variant	CDR-L1	CDR-L2	Fv Charge pH 7.4 (SMACK)	Fv HI (SMACK)	pI	MW Using Mass Spec (Da)
Ranibizumab (WT)	SASQDISNYLN	FTSSLHS	+0.1	1212	8.05 (meas.)	48380
RBZ-6	ITSTDIDDDMN	DTSDLES	-6.0	1152	6.05 (theor.)	48395
RBZ-3	SASQDISNYLN	DTSDLES	-3.0	1009	6.81 (meas.)	48368
RBZ-2.9	ITSTDIDDDMN	FTSSLHS	-2.9	1200	6.85 (theor.)	48407
RBZ+4.1	RARQGIRNYLN	FTSSLHS	+4.1	1122	9.38 (meas.)	48530
RBZ+7	RARQGIRNYLN	KTSRRHS	+7	1160	10.20 (meas.)	48623
RBZ less – hydro.	QASQDISNSLN	STSNLHS	+0.1	1165	8.85 (theor.)	48313
RBZ more – hydro.	SVSQVISSWLA	FASSLQT	+1.05	1296	9.05 (theor.)	48321

Figure 2. ***A, charge surface of ranibizumab WT. B, charge surface of RBZ-3. C, charge surface of RBZ+7.***

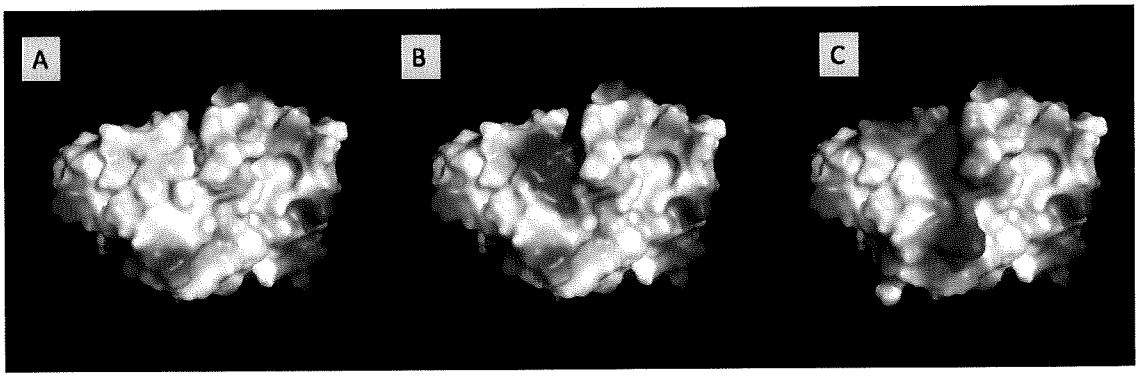

The bench scale cell culture showed extremely low expression rate for the charge variants, and less than 2.5mg of purified material could be obtained per liter of cell culture. As a result, material was purified from large-scale fermentation (10L) of the charge variants yielding sufficient quantities for further study. Intact mass spectroscopy confirmed that the purified Fabs had the expected molecular weights of 48380 Da, 48368 Da, and 48530 Da for ranibizumab WT, RBZ-3 and RBZ+7, respectively. A lower abundance fragment at ~35524Da was observed for all the samples.

SPR measurements were used to determine the affinities for binding of these Fabs to immobilized VEGF. As shown in **Table 3**, the VEGF-binding affinity of ranibizumab WT was similar to the previously reported value of 0.06 nM determined using a different format for the SPR assay[9]. The SPR measurements (**Table 3**) confirmed the charge variants retained high affinity binding to VEGF. We did observe differences in the response level for the variant Fabs injected at the same concentration onto the sensor chip having immobilized VEGF. In addition, slow kinetics of binding and dissociation were measured for Fabs interacting with immobilized VEGF making it uncertain if the affinity differences reported in **Table 2** for the variant Fabs are accurate. More experiments are required to provide an absolute ranking based on affinity; nonetheless, the VEGF-affinity of the variants is sufficient to use VEGF-binding ELISA as a detection method in pharmacokinetic studies.

Isoelectric point (pI) determination using icIEF (**Table 3**) confirmed the charge variant design with pI values ranging from 6.8 to 10.2.

Table 3. Properties of designed charge variants of ranibizumab

Molecule	CDR-L1	CDR-L2	pI	K_D VEGF-binding (nM)
Ranibizumab WT	SASQDISNYLN	FTSSLHS	8.0	0.24
RBZ-3	SASQDISNYLN	DTSDLES	6.8	0.02
RBZ+7	RARQGIRNYLN	KTSRRHS	10.2	4.3

In order to ensure that the product quality of the charge variants would not impact the result of the rabbit intravitreal PK study, a three-week 37°C incubation study was done at 10mg/mL in PBS, pH 7.4 for the ranibizumab charge variants. Over the three-week incubation study, acidic charge variants (**Figure 3**) of RBZ-3 increased from 6% to 21%. Acidic charge variants of RBZ+7 increased from 12% to 15%, the magnitude of the increase not being much greater than the variability in the method. For both variants, negligible increases in basic charge variants or high molecular weight species were observed in this study. These results are similar to that previously reported for ranibizumab (de Jong & Gikanga, Pharm Dev Memo 1486) with the exception that the rate of acidic charge variant generation is higher for the RBZ-3 protein. The sequence

changes in RBZ-3 would not be expected to influence a deamination site such that the origin of the increased rate of acidics generation is unknown. Nonetheless, the results of this short-term stability study indicate that the ranibizumab charge variants have sufficient stability for in vivo studies.

Figure 3. Product quality of the charge variants over a three-week 37°C incubation study

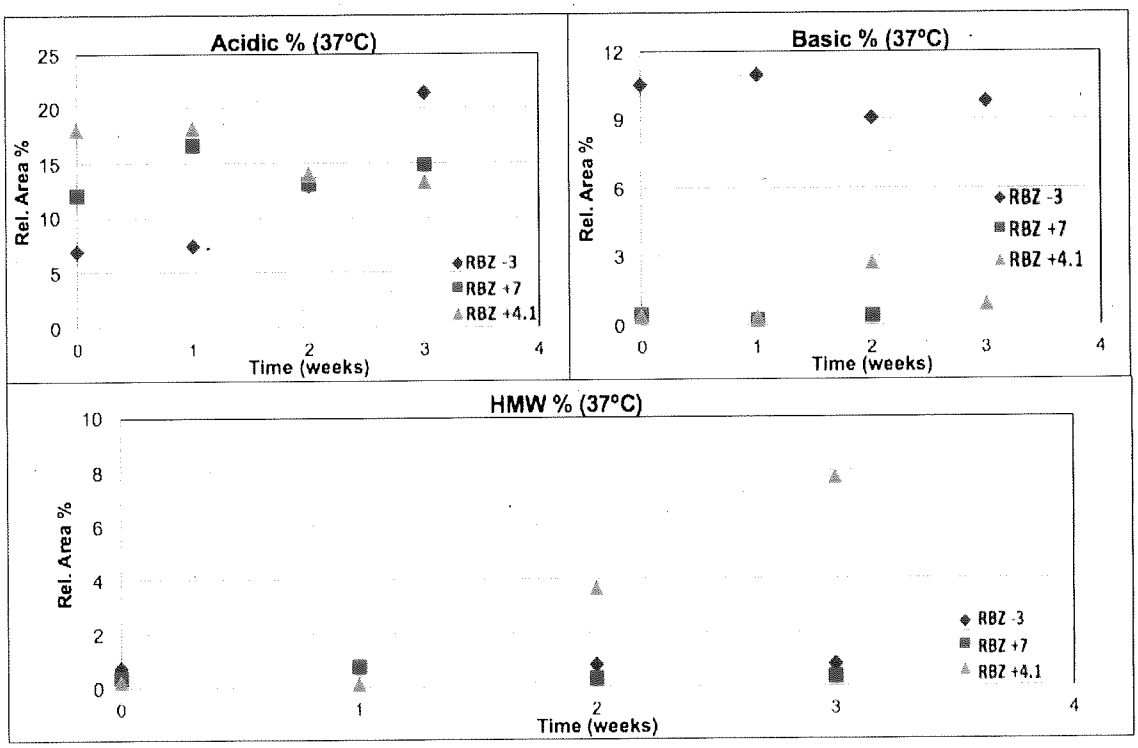

3.2 Ranibizumab hydrophobicity variants production and characterization

The design and production of the ranibizumab hydrophobicity variants were built upon the success of the ranibizumab charge variants study shown in section 3.1. Based on the high-

resolution crystal structure of the ranibizumab: VEGF complex[9], amino acid substitutions were made to CDR-L1 and CDR-L2 sequences in ranibizumab to generate one less (H-) and one more (H+) hydrophobic Fab variants. Using a sequence-based hydrophobicity index (HI) calculation for ranking, the range of the Fv HI was about 131 units between the H- and the H+ variants. In order to assess the impact of hydrophobicity on vitreal clearance and ocular partitioning specifically, the overall charge of the hydrophobicity variants was designed to be as close as possible to ranibizumab WT, having calculated Fv charge of +0.1 at pH 7.4, The less hydrophobic variant retains this charge profile whereas the more hydrophobic variant has a calculated Fv charge of +1.1, due to the Asp to Val change in CDR-L1. Similar to the charge variants design, since hydrophilic or hydrophobic amino acid sequences were introduced into adjacent CDRs, a H- or a H+ hydrophobic "patch" is produced rather than a delocalized hydrophobicity region. Intact mass spectroscopy confirmed the purified Fabs had the expected molecular weights of 48312 Da, and 48311 Da for the H- and the H+ hydrophobic variants, respectively. A low abundance fragment at ~35524Da was observed in the hydrophobicity variants, similar to that observed in the charge variants study.

Since the Fv HI is a calculated parameter and cannot be measured directly, an experiment was executed to correlate the sequence-based HI with an experimental measure of hydrophobicity such as elution position from a hydrophobic interaction column. As shown in **Figure 4**, Fv HI and elution time from a ProPacHIC-10 column appear to be correlated for

a panel of Fabs tested, suggesting that sequence-based HI calculation is a valid tool to design and rank Fabs regarding their relative hydrophobicity. One outlier was noted in that a Fab with calculated Fv HI of 1020 did not bind to the column in the loading buffer (95% A) and eluted in the flow-through fraction. This Fab also had a higher calculated negative charge compared to ranibizumab negative charge variants, and electrostatic repulsion could have prevented binding to the HIC resin.

Figure 4. Correlation of HIC elution time with hydrophobicity index calculated for Fv

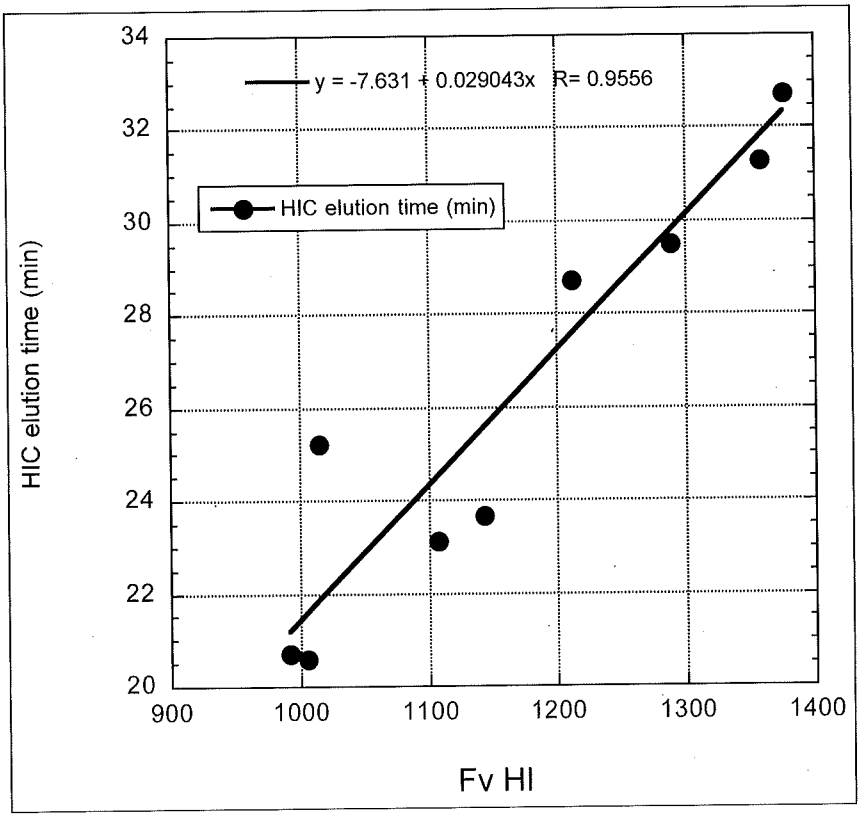

3.3 Intravitreal pharmacokinetics of ranibizumab charge variants

Mean vitreous concentration versus time profiles observed upon intravitreal injection of a 0.3 mg dose of ranibizumab WT, or its charge variants are shown in **Figure 5**. Consistent data with little inter-animal variability was observed out to 18 days. Results of non-compartmental analysis of these data indicate that both charge variants have a vitreal half-life (**Table 4**) of 3.0 days in comparison to 3.3 days determined for the comparator dose of ranibizumab. These half-life values are well within the normal inter-study range observed for ranibizumab WT (3.4 ± 0.7 days). Varying the overall charge of ranibizumab over a 10-unit range does not have a significant impact on vitreal half-life. A plot of vitreal half-life versus isoelectric point (**Figure 6**) for the Fabs listed in **Table 1** indicates that these parameters are not correlated. No trend in half-life with measured pI is observed. Similarly, varying the overall charge of ranibizumab has little effect on the pharmacokinetics observed for retinal tissue (**Table 5**) as the differences in calculated values for these Fabs are not greater than the standard errors. Results from multiple rabbit studies on ranibizumab indicate a range of 0.1-0.7 for the retina AUC/vitreous AUC ratio, a relative measure of drug exposure in the retina. A first approximation is that charge variation in ranibizumab does not affect retinal exposure; however, more precise measurements of retinal penetration are needed to make stronger conclusions about the effect of variation in molecule properties on distribution to the retina.

Table 4. Vitreous pharmacokinetic parameters for ranibizumab charge variants

Molecule	AUC_{all} (day*µg/mL)	Half-life (days)	CL (mL/day)	V_z (mL)	C_{max} (µg/mL)
Ranibizumab WT	822 ± 46.9	3.3	0.36	1.4	184 ± 20.7
RBZ+7	1090 ± 40.9	3.0	0.27	1.0	246 ± 11.1
RBZ-3	865 ± 76.6	3.0	0.34	1.2	219 ± 3.90

Figure 5. Vitreous concentration versus time profile for ranibizumab variants

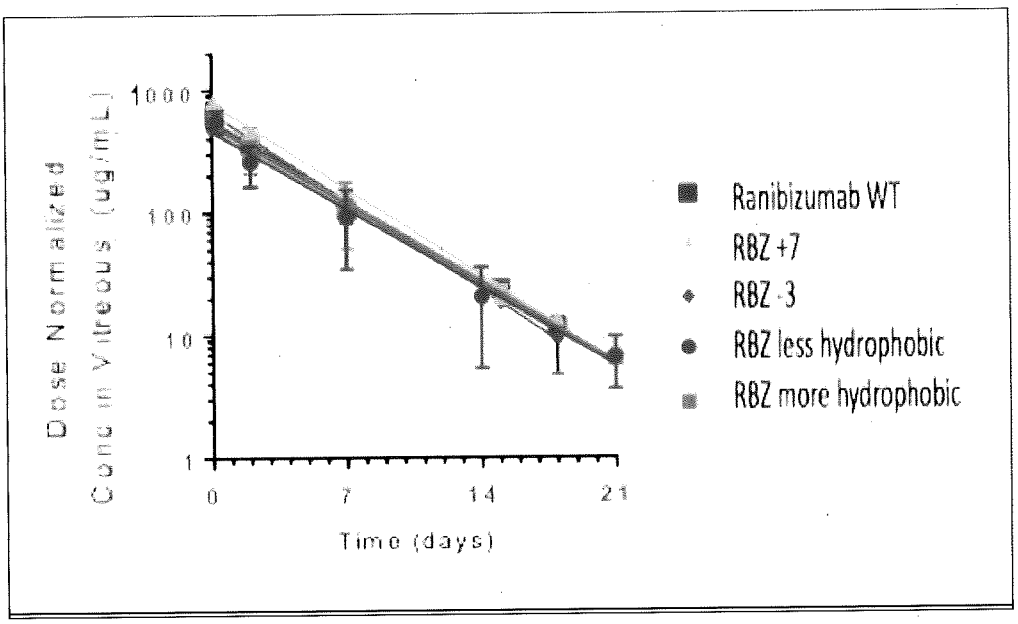

Figure 6. Correlation of vitreal half-life with isoelectric point (pI)

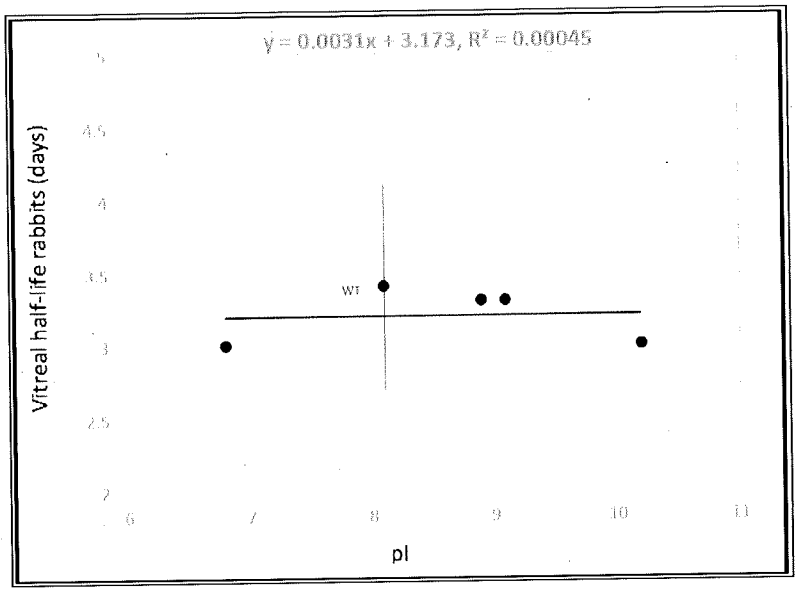

3.4 Intravitreal pharmacokinetics of ranibizumab hydrophobicity variants

Mean vitreous concentration versus time profiles observed upon intravitreal injection of a 0.5 mg dose of ranibizumab WT (average value from historical rabbit intravitreal PK studies), and the ranibizumab hydrophobicity Fab variants, are shown in

Figure 5. Over a 21-day rabbit intravitreal PK study, consistent vitreous data were obtained between the ranibizumab WT and the hydrophobicity variants (**Table 5**). Similar to the charge variants vitreous pharmacokinetic parameters, the half-life values of the hydrophobicity variants (3.1 to 3.3 days) are well within the normal inter-study range observed for ranibizumab WT (3.4 ± 0.7 days). Varying the overall hydrophobicity of ranibizumab over a 131-unit Fv HI range does not have a significant impact on vitreal half-

life. Vitreal half-life is not strongly correlated with sequence-based Fv HI (**Figure 7**). There is a weak trend of longer half-life with an increase in HI; nonetheless, the correlation coefficient is much less than one for a linear relationship between half-life and HI. Again, the range of half-life values is not greater than the inter-study variability determined for ranibizumab.

Table 5. Retina pharmacokinetic parameters for ranibizumab charge variants

Molecule	AUC_{all} (day*µg/mL)	Retina AUC/Vitreous AUC	Half-life (days)	C_{max} (µg/mL)
Ranibizumab WT	586±130	0.7	2.8	117±34.4
RBZ+7	581±222	0.5	3.1	170±80.0
RBZ-3	679±154	0.8	2.7	111±61.7

Figure 7. Correlation of vitreal half-life with Fv hydrophobicity

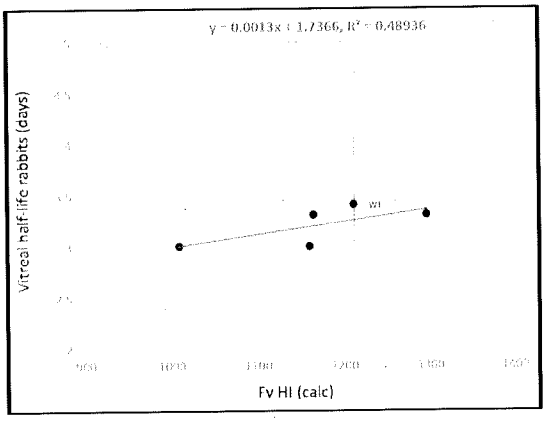

3.5 Relationship between vitreal half-life and hydrodynamic radius (R_H)

Previous studies done by Shatz et al. (2016)[5] showed that vitreal half-life in rabbits is linearly dependent on hydrodynamic radius (R_H), highlighting the contribution from diffusion within the vitreous chamber to the overall elimination rate. This relationship was initially established with a training set of 3 test articles with range in R_H and half-life of 2.5-6.9 nm and 3.2-6.1 days, respectively. As shown in ***Figure 8***, the linear relationship has been extended to include 13 samples, including ranibizumab, lampalizumab, albumin and 500 kD hyaluronic acid[7], over a R_H range of 2.5 nm – 45 nm. The linear dependence of rabbit vitreal half-life on R_H is maintained with good correlation (R=0.9935) over this expanded range of R_H values.

Figure 8. Correlation of vitreal half-life with hydrodynamic radius (R_H)

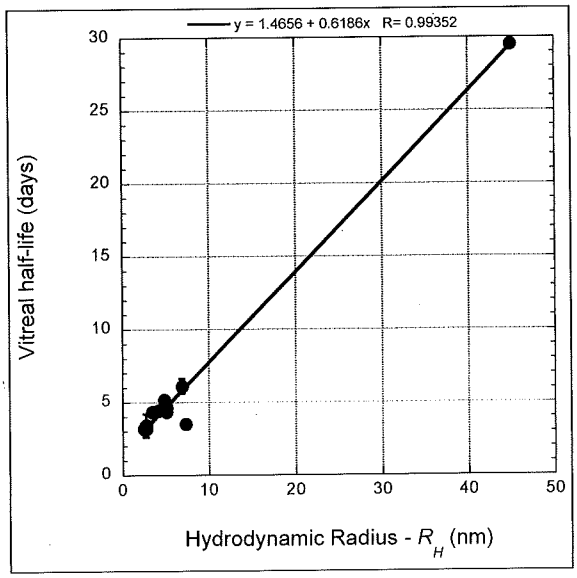

4. DISCUSSION

While many researchers have used surface modified nanoparticles as a probe to study the diffusivity and permeability of drug molecules in vitreous and across retina after intravitreal injection, the impact of physicochemical properties such as hydrodynamic size, electrostatic charge, and hydrophobicity on the vitreal PK of protein therapeutics have yet to be studied.

Here, we executed two systematic studies, where molecular charge or molecular hydrophobicity was varied by introducing point mutations into ranibizumab. It should be noted that it is challenging to manipulate charge through amino acid substitutions without altering hydrophobicity. For example, introduction of acidic residues into CDR-L2 to lower the pI also decreases the calculated hydrophobicity, in RBZ-3 charge variant where mutation resulted in a lower pI (6.81) and hydrophobicity (1009 Fv HI) than ranibizumab WT (8.05 in pI and 1212 in Fv HI). On the other hand, it is easier to maintain the overall charge of the Fab variants, when manipulating the amino acid sequence on CDR-L1 and CDR-L2 to vary ranibizumab's hydrophobicity. For example, introduction of more hydrophilic residues provided a variant with the same calculated pI value (8.9) as ranibizumab WT. The H- and H+ hydrophobic variants provide a sufficient range (131 units) of hydrophobicity variation, with a Fv charge variation of only 1 unit.

Results of pharmacokinetic studies (**Table 4**) suggest that negatively and positively charged variants have vitreal half-life equivalent to ranibizumab WT. Ranibizumab WT, RBZ-3 and RBZ+7 also have similar pharmacokinetics in the retina suggesting that pI variation in this range (6.8-10.2) does not affect distribution to retina tissue. The introduction of ionizable residues into adjacent CDRs results in clustered rather than more dispersed charge. It is unknown if a different result would be obtained if an approach for introducing de-localized charge variation in ranibizumab was used.

Leveraging the knowledge of the systematic charge study, the hydrophobicity study was designed to determine pharmacokinetic parameters for ranibizumab variants comprising hydrophobic amino acid substitutions in CDRs L1 and L2. The result shown in **Table 6** suggested that H- and H+ hydrophobic variants have equivalent vitreal half-life as ranibizumab WT Vitreal half-life in rabbit does not appear to be dependent on Fv hydrophobicity calculated from the amino acid sequence (**Figure 7**). The calculated hydrophobicity index (Fv HI) seems to provide a reasonable estimate of the overall hydrophobicity of native Fabs since elution position from a hydrophobic interaction column (HIC) is correlated with Fv HI (**Figure 4**).

Table 6. Vitreous pharmacokinetic parameters for ranibizumab hydrophobicity variants

Molecule	AUC_inf/D (µg/mL*d/mg)	Half-life (days)	CL (mL/day)	Vz (mL)	Cmax/D (µg/mL/mg)
Ranibizumab WT	2220	3.1	0.45	2.0	500 ± 30
RBZ less hydro.	2530	3.3	0.40	1.9	580 ± 60
RBZ more hydro.	2550	3.3	0.39	1.8	570 ± 30

Results from multiple rabbit pharmacokinetic studies conducted at Genentech on four antibody Fabs and one Mab of diverse binding targets has been summarized in **Figure 9** and **Figure 10**. The comparison study was performed to identify the relationships between vitreous volume of distribution or clearance, with pI (5.1 - 10.2) or Fv HI (1004-1358). The tightly distributed comparison plots with linear regression R^2 values much lower than one suggested that vitreal PK in rabbits of all Fabs regardless of target is not strongly correlated with Fv hydrophobicity index (FvHI) or isoelectric point (pI). Furthermore, one of the Fab charge variants series included in the comparison was accomplished by changing both the CDR and framework regions of the molecule such that charge differences are more spread out[10]. The clustered summary plots suggest that diffuse and clustered charge variants are equivalent.

Figure 9. Relationships between the vitreous volume of distribution or clearance, and pI in rabbit for five charge and hydrophobicity series

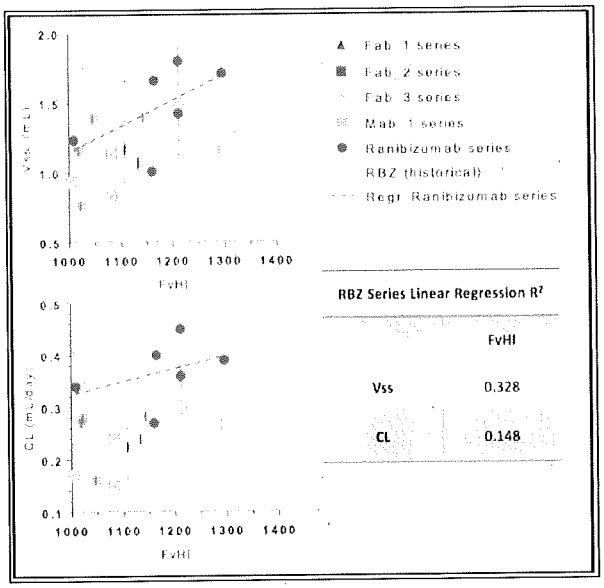

Figure 10 Relationships between the vitreous volume of distribution or clearance, and Fv HI in rabbit for five charge and hydrophobicity series

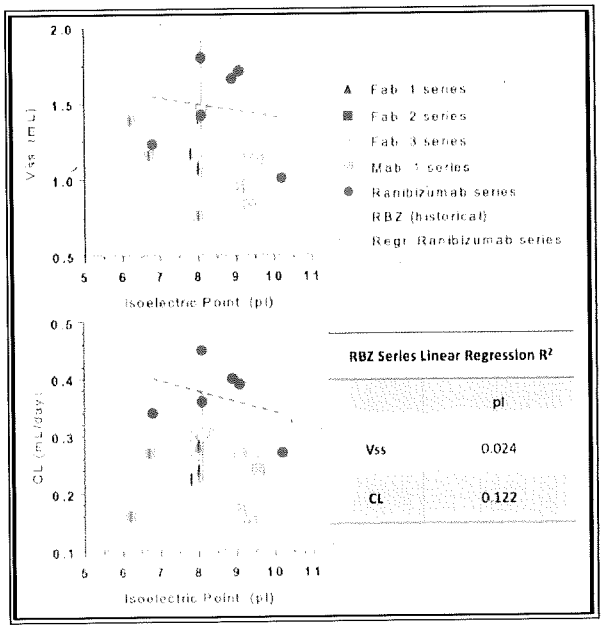

The diffuse and clustered charge pattern on Fab variants can provide different charge-charge interactions between the charge variants and the collagen-hyaluronic acid (HA - negatively charged mega Da molecule[24]) network in vitreous. For example, if charge pattern on the charge variant is complimentary to the electrostatic surface of HA, a charge-charge interaction could potentially extend the vitreal half-life of electropositive variants. The half-life values determined for high pI molecules suggests that electrostatic interaction with vitreous structure in rabbit is negligible for the molecules studied in this report.

Limited pharmacokinetic data in non-human primate is available to assess the influence of molecule properties on vitreal half-life and thus translation to behavior expected in human is unknown. Four antibody Fabs (pI range 7.6-9.3) have been assessed for ocular pharmacokinetics in cynomolgus monkey at Genentech and the range in vitreal half-life (2.3-2.7 days) between molecules is not significantly greater than the inter-study variability. Pharmacokinetic data in humans after intravitreal injection is available for ranibizumab and lampalizumab from analysis of drug levels in aqueous humor[11] or serum[12], respectively. After considering variability in patient population and sampling method, it can be concluded that the rate of elimination of ranibizumab and lampalizumab from the vitreous body is equivalent. Since these molecules have similar pI values, but differ in the distribution of charge, there is insufficient data to make solid conclusions about the role of molecular charge in human ocular pharmacokinetics. Nonetheless, a reasonable expectation from

studies in other species is that variation in charge for antibody Fabs will have inconsequential effects for human vitreal half-life.

Hydrodynamic size is a key variable for estimation of vitreal half-life and reflects diffusion within the vitreous chamber as the rate determining step in elimination[5, 13, 14]. Vitreal half-life in rabbit can be predicted from measurements of hydrodynamic radius and using solely the linear relationship shown in **Figure 8** while ignoring contributions from other attributes. There is insufficient understanding to predict vitreal half-life in human from R_H measurements; nonetheless, differences in human half-life between Macugen® (R_H =7.3 nm, human $t_{1/2}$=10 days[6]) and lampalizumab (R_H =2.8 nm, human $t_{1/2}$=5.9 days[12]) are consistent with a similar dependence of human vitreal half-life on hydrodynamic size. While more studies in other species are required to build an effective model for prediction of human ocular pharmacokinetics, estimates of half-life can be made using measurements of hydrodynamic size alone.

Our results are not consistent with conclusions made from studies of nanoparticles with charge or hydrophobicity surface modification[15,16,17]. In contrast to results of nanoparticle studies, we find that vitreal half-life of Fabs, regardless of target, is not correlated with hydrophobicity or electrostatic charge. The opposing result hinted that the impact of

overall charge or hydrophobicity can still be important, but may only be evident for larger particles or for higher charge densities. A hydrodynamic size threshold might exist to govern the contribution of these physicochemical properties to vitreal clearance. The common hydrodynamic size range of surface modified nanoparticle was between 200 – 300 nm[16, 17], which is about 100 times larger than our ranibizumab Fab molecule probe (R_H = 2.8nm). Furthermore, the range of electrostatic charge in Fv covered in the ranibizumab charge variants was -3 to +7, which is more limited compared to many studies of charge modified nanoparticles. In addition, a quantitative understanding of the impact of variation in molecule attributes on retinal penetration is less well developed. Although charge variation in ranibizumab does not appear to affect retinal exposure, current approaches to measure this parameter have high variability. Effects of hydrophobic variation in ranibizumab on retinal exposure have not yet been determined. Taken together, further study of the impact of physicochemical properties on the ocular PK and distribution of large molecules is warranted.

Using protein engineering to enhance the chemical and physical stability of molecules is becoming more important for the development of ocular long-acting delivery (LAD) technologies. Charge or hydrophobicity variants resulting from structure-guided amino acid substitutions are usually designed to not only improve chemical and physical stability, but

retain equivalent or improved pharmacokinetics properties (such as: vitreal half-life, vitreous to retina penetration, etc.). The result from the two systematic studies suggest that charge or hydrophobicity variants with a better chemical and physical stability and equivalent pharmacokinetics parameters is achievable with Fab molecules. Using amino acid substitutions, molecules can be designed to retain sufficient antigen-binding capacity over a longer period of time by eliminating isomerization, deamidation and fragmentation sites to reduce charge species and fragment formation. Such engineering facilitates the application of long-acting delivery technologies that enable better treatment options for patients.

5. CONCLUSIONS

On the basis of retrospective and systematic pharmacokinetics studies in rabbits, it is concluded that variation in molecular charge and hydrophobicity appears to have only a minor influence on vitreal half-life. The linear regressions done on a range of antibody Fabs confirmed that no signification correlation exists between vitreous volume of distribution or clearance, and FvHI or pI in rabbit within the pI range of 5.4 - 10.2 and Fv HI range of 1004 – 1358. The results support our hypothesis that hydrodynamic size is a key determinant of vitreal clearance whereas minor or negligible contributions are provided by variation in molecule charge and hydrophobicity.

Although results of fewer studies in other species are available to aid translation, similar behavior is expected for vitreal half-life in human. Chemical instabilities that produce charge variants with pI values in the range (5.4-10.2) tested in this report are not expected to cause significant differences in vitreal half-life. Similarly, the magnitude of hydrophobic variation that can result from chemical degradation would be too small to affect vitreal half-life. Finally, hydrodynamic size is a key variable for ocular pharmacokinetics and increasing the hydrodynamic radius of a molecule can slow vitreal clearance.

6. REFERENCES

1. Lim LS, Mitchell P, Seddon JM, Holz FG, Wong TY. Age-related macular degeneration. Lancet 2012; 379:1728-38.

2. Brown DM, Kaiser PK, Michels M, Soubrane G, Heier JS, Kim RY, et al. Ranibizumab versus verteporfin for neovascular age-related macular degeneration. The New England journal of medicine 2006; 355:1432-44.

3. Rosenfeld PJ, Brown DM, Heier JS, Boyer DS, Kaiser PK, Chung CY, et al. Ranibizumab for neovascular age-related macular degeneration. The New England journal of medicine 2006; 355:1419-31.

4. Wong WL, Su X, Li X, Cheung CM, Klein R, Cheng CY, et al. Global prevalence of age-related macular degeneration and disease burden projection for 2020 and 2040: a systematic review and meta-analysis. Lancet Glob Health 2014; 2:e106-16.

5. Shatz W, Hass PE, Mathieu M, Kim HS, Leach K, Zhou M, et al. Contribution of Antibody Hydrodynamic Size to Vitreal Clearance Revealed through Rabbit Studies Using a Species-Matched Fab. Molecular pharmaceutics 2016; 13:2996-3003.

6. Apte RS, Modi M, Masonson H, Patel M, Whitfield L, Adamis AP. Pegaptanib 1-year systemic safety results from a safety-pharmacokinetic trial in patients with neovascular age-related macular degeneration. Ophthalmology 2007; 114:1702-12.

7. Laurent UB, Fraser JR. Turnover of hyaluronate in the aqueous humour and vitreous body of the rabbit. Experimental eye research 1983; 36:493-503.

8. Salas-Solano O, Kennel B, Park SS, Roby K, Sosic Z, Boumajny B, et al. Robustness of iCIEF methodology for the analysis of monoclonal antibodies: an interlaboratory study. J Sep Sci 2012; 35:3124-9.

9. Chen Y, Wiesmann C, Fuh G, Li B, Christinger HW, McKay P, et al. Selection and analysis of an optimized anti-VEGF antibody: crystal structure of an affinity-matured Fab in complex with antigen. Journal of molecular biology 1999; 293:865-81.

10. Li B, Tesar D, Boswell CA, Cahaya HS, Wong A, Zhang J, et al. Framework selection can influence pharmacokinetics of a humanized therapeutic antibody through differences in molecule charge. mAbs 2014; 6:1255-64.

11. Xu L, Lu T, Tuomi L, Jumbe N, Lu J, Eppler S, et al. Pharmacokinetics of ranibizumab in patients with neovascular age-related macular degeneration: a population approach. Investigative ophthalmology & visual science 2013; 54:1616-24.

12. Do DV, Pieramici DJ, van Lookeren Campagne M, Beres T, Friesenhahn M, Zhang Y, et al. A phase ia dose-escalation study of the anti-factor D monoclonal antibody fragment FCFD4514S in patients with geographic atrophy. Retina 2014; 34:313-20.

13. Missel PJ. Simulating intravitreal injections in anatomically accurate models for rabbit, monkey, and human eyes. Pharmaceutical research 2012; 29:3251-72.

14. Hutton-Smith LA, Gaffney EA, Byrne HM, Maini PK, Schwab D, Mazer NA. A Mechanistic Model of the Intravitreal Pharmacokinetics of Large Molecules and the Pharmacodynamic Suppression of Ocular Vascular Endothelial Growth Factor Levels by Ranibizumab in Patients with Neovascular Age-Related Macular Degeneration. Molecular pharmaceutics 2016; 13:2941-50.

15. Joyce Mordenti, R. Andrew Cuthbertson, et al. Comparisons of the intraocular Tissue Distribution Pharmacokinetics, and Safety of ^{125}I-Labeled Full-Length and Fab Antibodies in Rhesus Monkeys Following Intravitreal Administration. Toxicologic Pathology 1999; 27:536-544.

16. Heebeom Koo, Hyungwon Moon, et al. The movement of self-assembled amphiphilic polymeric nanoparticles in the vitreous and retina after intravitreal injection. Biomaterial 2012; 33:3485-3493

17. Binapani Mahaling, Dhirendra S. Katti, et al. Understanding the influence of surface properties of nanoparticles and penetration enhancers for improving bioavailability in eye tissue in vivo. International Journal of Pharmaceutics 2016; 501:1-9.

18. David Maurice, Review: Practical Issues in Intravitreal Drug Delivery. Journal of Ocular Pharmacology and Therapeutics 2001, 17:4.

19. Durairaj, C.; Shah, J.; Senapati, S.; Kompella, U., et al. Prediction of vitreal half-life based on drug physicochemical properties: quantitative structure - pharmacokinetic relationships (QSPKR), Pharmaceutical Research 2009; 26:1236-1260.

20. Gaudana, R.;Ananthula, H.; Parenky, A.; Mitra, A., et al. Ocular Drug Delivery, AAPS J 2010, 12.

21. Le Goff, et al. Adult vitreous structure and postnatal changes. Eye 2008; 22:1214-1222.

22. Sebag, J; Yee, Kenneth MP, et al. Chapter 16 Vitreous: From Biochemistry to Clinial Relevance 2007.

23. Xu W, Boylan NJ, et al. Nanoparticle diffusion in , and microheology of, the bovine vitreous ex vivo. Journal of Controlled Release 2013; 167:76-84

24. Noulav AV, Skandalis SS, et al. Variations in content and structure of glycosaminoglycans of the vitreous gel from different mammalian species. Biomed Chromatography 2004; 18:457-61.

25. Elsenberg D, McLachian AD, Solvation energy in protein folding and binding. Nature 1986: 319:199-203.

26. McConnell MJ, Pachon J, Expression, purificaiton, and refolding of biologically active Acinetobacter baumannii OmpA from Escherichia coli inclusion bodies. Protein Expreesion Purification 2011; 77:98-103.

27. Jay S. Bolden, Rob E. Warburton, et al. Endotoxin recovery using limulus amebocyte lysate (LAL) assay. Biologicals 2016; 44:434-440.

28. Mihai Pop, Steven L. Salzberg, Bioinformatics challenges of new sequencing technology, CellPress 2008; 24:142-149.

29. Couto MR, Rodrigues JL, Rodrigues LR, Optimization of fermentation conditions for the production of curcumin by engineered Escherichia coli. J R Soc Interface 2017; 14:133.

30. Eva M. del Amo, Anna-Kaisa Rimpela, et al. Pharmacokinetic aspects of retinal drug delivery, Progress in Retinal and Eye Research 2017; 57:134-185.